Biochemical and Biophysical Research Communications 431 (2013) 376–381

Contents lists available at SciVerse ScienceDirect

Biochemical and Biophysical Research Communications

journal homepage: www.elsevier.com/locate/ybbrc

The X-ray crystal structure of PA1374 from *Pseudomonas aeruginosa*, a putative oxidative-stress sensing transcriptional regulator

Hyunjin Kim, Jungwoo Choe *

Department of Life Science, University of Seoul, Seoul 130-743, Republic of Korea

ARTICLE INFO

Article history:
Received 4 January 2013
Available online 18 January 2013

Keywords:
Transcriptional regulator
Oxidative stress
MarR family
Crystallography

ABSTRACT

Members of the multiple antibiotic resistance regulator (MarR) family regulate the expression of genes related to antibiotic resistance, oxidative stress, and virulence in bacteria and Archaea. Here, we determined the structure of PA1374 from *Pseudomonas aeruginosa* at 2.3 Å resolution. PA1374 belonged to the MarR family and its structure revealed a tightly bound dimer with each subunit containing a winged helix–turn–helix (wHTH) DNA-binding motif. Conserved arginine residues, Arg55, Arg74, and Arg77, were located in the wHTH region, which might be important to DNA binding. Furthermore, each monomer contained a pocket made of conserved hydrophobic residues. A highly conserved Cys11 located at one end of this pocket may undergo oxidation by organic hydroperoxide molecules, as shown in other MarR family proteins acting as redox-sensing regulators. These results provide insights about the role of PA1374 as a putative oxidative-stress sensing transcriptional regulator.

© 2013 Elsevier Inc. All rights reserved.

1. Introduction

Upon bacterial infection, the host innate immune system generates reactive oxygen species (ROS) as a defense mechanism. Accordingly, it is not surprising that many bacteria have developed oxidation-sensitive regulators to survive oxidative stress [1]. The majority of ROS-sensing systems employ highly conserved cysteine residues that are oxidized by ROS, leading to conformational changes and transcriptional activity [2,3]. The organic hydroperoxide resistance regulator (OhrR) protein, a member of the MarR family, is a transcriptional repressor that responds to oxidative stress caused by organic hydroperoxides (OHPs) [4,5]. For example, *Xanthomonas campestris* OhrR undergoes oxidation of a reactive cysteine residue close to the N-terminus upon exposure to OHPs such as linoleic acid hydroperoxide, followed by the formation of intersubunit disulfide bonds and conformational changes [6]. These changes lead to the release of OhrR from DNA and expression of thiol peroxidases, which reduce OHPs to less harmful alcohols [7,8]. OhrR family proteins can be divided into the 2-cysteine family as in *X. campestris* and the 1-cysteine family as in *B. subtilis* [4]. The binding affinity of *B. subtilis* OhrR, a member of the 1-cysteine family, to its cognate DNA was reduced by the oxidation of a single conserved cysteine residue located near the N-terminus to the corresponding cysteine–sulfenic acid, and perhaps to higher oxidation states [9].

Here, we describe the crystal structure of *P. aeruginosa* PA1374, a homodimer with a large dimer interface including three antiparallel β-sheets made of β-strands from both subunits. Structure analysis revealed that PA1374 contained a wHTH motif in which conserved Arg residues located in the recognition helix as well as the loop in the wing region can interact with the major and minor grooves of DNA, respectively. Further, PA1374 contained a highly conserved Cys11 located nearby a hydrophobic pocket that may undergo oxidation by OHPs, as shown in other OhrR family proteins. Based on the presence of a wHTH motif and hydrophobic pocket close to a highly conserved cysteine, we propose that *P. aeruginosa* PA1374 is an oxidative stress sensor of OHPs.

2. Materials and methods

2.1. Cloning, protein preparation, and purification

The *PA1374* gene was amplified from *P. aeruginosa* genomic DNA by polymerase chain reaction (PCR) using primers (5′-TACTTCCAATCCAATGCAATG CAACGCAAGACCTTCGC-3′, 5′-TTATCCACTTCCAATGTTATCATCGAGCCGGTA-GCTCG-3′). The purified PCR product was cloned into pLIC-Tr3Ta-HA vector containing an N-terminal His_6-tag and TEV protease cut site. After TEV protease treatment, three amino acids (SNI) from the vector sequence were left in the N-terminus of PA1374 protein. The construct was transformed into BL21(DE3) *E. coli* strain (Novagen). Cells were grown in M9 medium containing 30 μg/mL of carbenicilin at 37 °C until an OD_{600nm} of 0.6, after which an amino acid mixture (100 mg/L each of Lys, Phe, and Thr; 50 mg/L each of Ile, Leu, Val, and Sel-Met) was

* Corresponding author. Address: 90 Jeonnong-dong, Dongdaemun-gu, Seoul 130-743, Republic of Korea. Fax: +82 2 2210 2888.
E-mail address: jchoe@uos.ac.kr (J. Choe).

0006-291X/$ - see front matter © 2013 Elsevier Inc. All rights reserved.
http://dx.doi.org/10.1016/j.bbrc.2013.01.044

added 30 min before induction with 1 mM isopropyl β-D-1-thiogalactopyranoside (IPTG). Growth was continued for 15 h at 18 °C, after which cells were harvested by centrifugation and lysed by sonication in 20 mM Tris–HCl (pH 7.5) and 250 mM NaCl buffer (lysis buffer). The lysate was then cleared by centrifugation, after which the supernatant was loaded onto a Ni-Sepharose 6 affinity column and eluted with a stepwise gradient of 50–400 mM imidazole in lysis buffer. After the N-terminal His_6-tag from the vector was cut by TEV protease at 4 °C, PA1374 was further purified using a Superdex75 size-exclusion column (GE Healthcare) equilibrated with a buffer composed of 20 mM Tris–HCl, 200 mM NaCl, 2 mM dithiothreitol, and 2 mM EDTA. Purity of the protein was analyzed by 15% sodium dodecyl sulfate–polyacrylamide gel electrophoresis.

2.2. Crystallization, data collection, and structure determination

Purified PA1374 was concentrated to 12.2 mg/mL by centrifugal ultrafiltration (Amicon). Crystals of PA1374 were obtained by the hanging-drop vapor-diffusion method at 20 °C using a well solution composed of 5.9% polyethylene glycol (PEG) 3350, 0.1 M sodium chloride, 0.1 M phosphate-citrate (pH 3.6), and 25% glycerol. Crystals were then transferred into a cryoprotectant solution composed of 5.9% polyethylene glycol (PEG) 3350, 0.1 M sodium chloride, 0.1 M phosphate–citrate (pH 3.6), and 30% glycerol and flash-frozen in liquid nitrogen. X-ray diffraction data were collected at a resolution of 2.3 Å at Photon Factory beamline BL-5A (Japan). Data were processed with HKL2000 [10], and an initial model of PA1374 was obtained using the Phenix program [11] with the peak and edge dataset. The space group was C2, and the asymmetric unit contained 12 subunits. The Matthews coefficient (Vm) was 2.4 $Å^3$/Da, and the estimated solvent content of the crystal was 48.8%. The model was refined with REFMAC [12], and manual model building was performed using the COOT program [13]. Two hundred ninety-nine residues out of 2016 were not observed in the electron density and were thus not included in the final model. The Ramachandran plot produced by PROCHECK showed that 97.4% of the residues are in the most favored and 2.6% in the favored region [14]. Data collection and refinement statistics are summarized in Table 1. Coordinate and structure factors of *P. aeruginosa* PA1374 have been deposited in the RCSB Protein Data Bank with accession code 4GCV.

3. Results and discussion

3.1. Overall structure

The structure of *P. aeruginosa* PA1374 was determined to 2.3 Å resolution by the multiple-wavelength anomalous dispersion method using selenomethionine-substituted protein crystals. The crystals belonged to the space group C2, and the asymmetric unit contained 12 subunits (or six dimers) of PA1374. The root-mean-square deviation (RMSD) between the 12 subunits in the asymmetric unit ranged from 0.55 Å to 1.03 Å, indicating that they shared very similar structures. The overall structure of PA1374 contained a winged–helix–turn–helix DNA binding motif formed by helices α3 and α4 as well as β strands β1 and β2, which is similar to those of other MarR family proteins (Fig. 1A). The β strands β1 and β2 formed an anti-parallel β-sheet with a connecting loop region containing conserved Arg residues for DNA binding [15,16]. The structure of PA1374 consisted of six α-helices, six β-strands, and one single-turn 3_{10} helix defined by DSSP [17] with the following topology: α1 (residues 11–20), α2 (residues 22–34), α3 (residues 38–47), α4 (residues 11–20), β1 (residues 66–70), β2 (residues 78–82), α5 (residues 83–10), β3 (residues 112–115), β4 (residues 123–129), β5 (residues 132–135), 3_{10} (residues 137–139), β6 (residues 140–143), and α6 (residues 150–156) (Fig. 1C).

PA1374 formed tightly intertwined dimer with a buried surface area of 3463 $Å^2$, which is 32% of the solvent accessible surface area (ASA) of each monomer [18]. This dimerization interface is the largest among all known MarR family member proteins (Table 2). The dimer interface involved 85 residues with 52 hydrogen bonds, 16 salt bridges, and numerous hydrophobic interactions. The major dimerization interface included helices α1, α4, α5, and α6 as well as β-strands β3, β4, β5, and β6. There were three anti-parallel β-sheets in the dimer interface formed by β3 (subunit A) and β6′ (subunit B), by β4, β5, β4′, and β5′, and by β6 and β3′. These anti-parallel β-sheets contributed 22 hydrogen bonds and two salt bridges to the dimer interface. Hydrophobic residues such as

Table 1
Data collection and refinement statistics.

	Peak	Edge
Data collection statistics		
Wavelength (Å)	0.97919	0.97937
Space group	C2	C2
Unit cell dimensions	a = 128.90	a = 129.06
	b = 74.45	b = 74.58
	c = 230.49	c = 230.80
	β = 90.03 Å	β = 90.02 Å
Resolution (Å)[a]	30.0–2.30 (2.34–2.30)	30.0–2.30 (2.34–2.30)
Observed reflections	1,718,940	1,707,264
Unique reflections	96,489	96,909
Completeness (%)	99.4 (99.2)	99.4 (99.2)
R_{sym} (%)[b]	0.070 (0.633)	0.047 (0.797)
I/σ (I)[c]	40.4 (2.9)	26.5 (2.3)
Refinement statistics		
No. of Residues	1717	
R_{cryst} (%)/R_{free} (%)[d]	21.4/28.7	
RMSD bonds (Å)	0.016	
RMSD angles (°)	1.771	

[a] Resolution range of the highest shell is listed in parentheses.
[b] $R_{sym} = \sum | I - \langle I \rangle | / \sum I$, where I is the intensity of an individual reflection and $\langle I \rangle$ is the average intensity over symmetry equivalents.
[c] $I/\sigma(I)$ is the mean reflection intensity/estimated error.
[d] $R_{cryst} = \sum || F_0 | - | F_c || / \sum | F_0$, where F_0 and F_c are the observed and calculated structure factor amplitudes, R_{free} is equivalent to R_{cryst} but calculated for 5% randomly chosen set of reflections that were omitted from the refinement process.

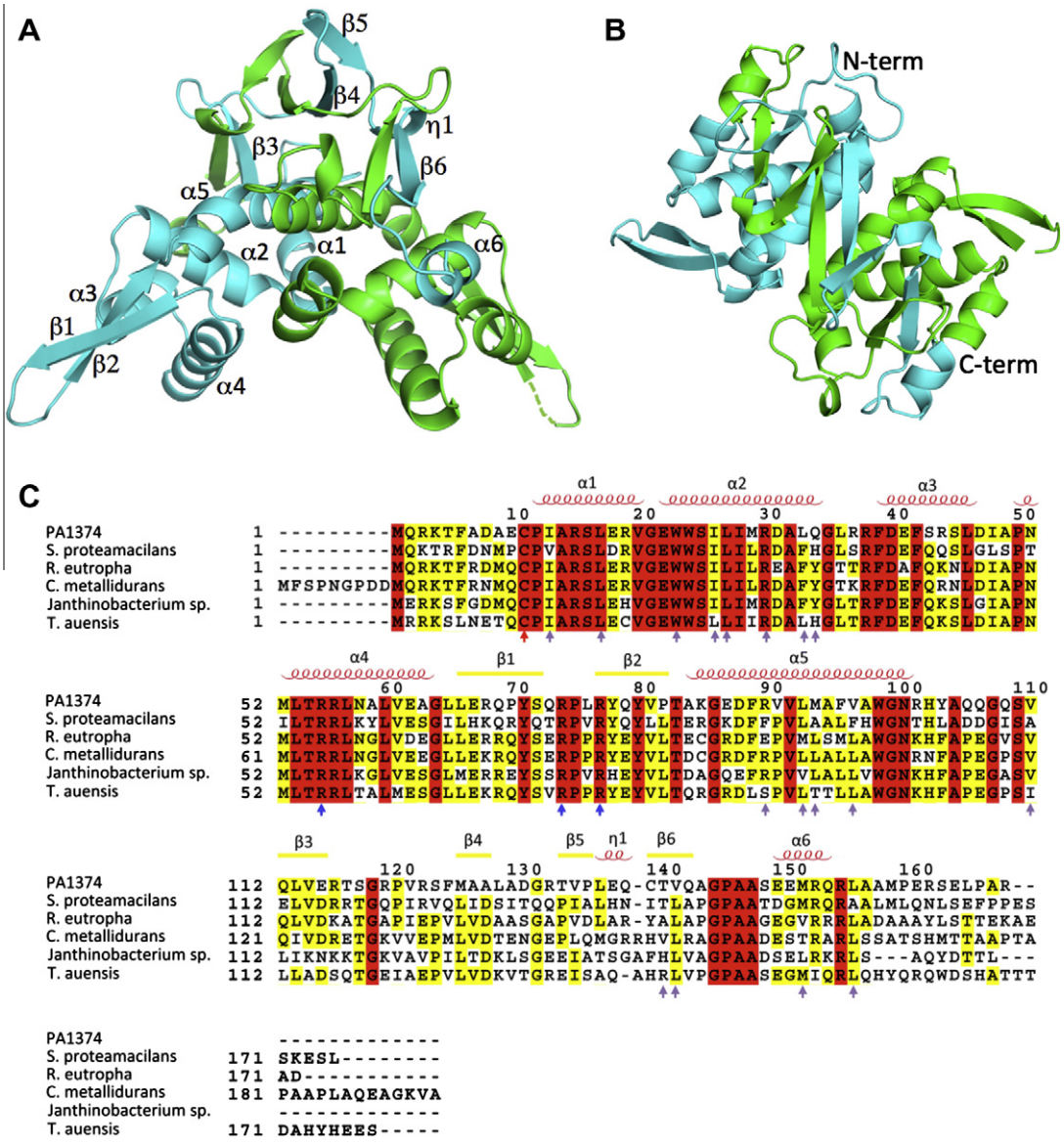

Fig. 1. Overall structure of PA1374 homodimer. (A) Overall structure of *P. aeruginosa* PA1374 dimer with one subunit colored in cyan and the other subunit in green. Secondary structure elements of the cyan subunit are labeled. (B) 90° rotated (top view) of (A). The N- and C-terminus of the cyan subunit are labeled. (C) Multiple sequence alignment of homologous sequences identified by BLAST search. The secondary structure elements of PA1374 are shown as α for alpha helix, β for β strand and η for 3_{10} helix. Residues that are identical in homologs are colored in red, highly conserved amino acids in yellow. Cysteine 11 of PA1374 is indicated with red arrow, arginine residues that can interact with DNA are marked with blue arrows and residues that form the hydrophobic pocket with purple arrows. The proteins used for the alignment are from the following organisms: PA1374, *Pseudomonas aeruginosa*; *S. proteamacilans, Serratia proteamaculans*; *R. eutropha, Ralstonia eutropha*; *C. metallidurans, Cupriavidus metallidurans*; *Janthiniobacterium sp., Janthinobacterium sp. Marseille*; and *T. auensis, Tolumonas auensis*. (For interpretation of the references to colour in this figure legend, the reader is referred to the web version of this article.)

Val20, Phe89, Val91, Val92, Phe96, Trp99, Leu113, Val122, Phe125, and Leu137 formed hydrophobic interactions in the center of the dimer. Among these hydrophobic residues, Val20, Val92, and Trp99 were completely conserved between homologous proteins, whereas Phe89, Val91, Phe96, Leu113, and Val122 were substituted with other hydrophobic residues (Fig. 1C).

3.2. Structural comparison

A search of structurally related proteins using the monomer of PA1374 using the DALI server [19] found five proteins with a Z-score higher than 10 with RMSDs ranging from 2.5 Å to 3.9 Å (Table 3). These proteins were identified as putative transcription factors from *P. aeruginosa* (PDB ID: 2F2E) [20], hypothetical transcriptional regulator from *Sulfolobus tokodaii* (2YR2), transcriptional repressor from *Methanobacterium thermoautotrophicum* (3BPV) [21], putative transcriptional regulator YtcD from *B. subtilis* (2HZT), and redox-sensing regulator HypR from *B. subtilis* (4A5 M) [2]. All of these proteins are transcription factors with wHTH DNA-binding motifs. Although the structures of the monomers are similar, their orientations in the dimer are quite variable [20]. 2F2E, another putative transcription factor from *P. aeruginosa* shared similar dimeric organization with PA1374 (Supplementary Fig. 1). 2YR2 and 3BPV, although similar in size (both of them with 146 amino acids, compared to PA1374 with 168 amino acids), showed quite different dimer structures and their RMSD's with PA1374 were 16.98 and 14.02 Å, respectively, when dimers were used for the superposition. 2HZT and 4A5M consist of 126, and 125 amino acids, respectively, and they superpose to the N-terminal part (from N-terminus to the α5 region) of PA1374. It is

Table 2
Comparison of dimerization parameters.

Protein	Area[a]	% Area[a]	# Residues[a]	H-bond[a]	Salt[a]
4GCV	3463	32	85	52	16
2F2E	3204	31	72	34	10
2YR2	3148	31	63	16	16
3BPV	2390	23	54	10	16
2HZT	1423	21	39	6	1
4A5M	1421	22	38	6	1

[a] Column headings refer to the following: (Area) The solvent accessible surface area of an individual monomer buried in the dimer interface (Å2); (% Area) the percentage of total monomer solvent accessible surface area found in dimer interface; (# Residues) the number of residues of a monomer involver in dimerization; (H-bond) the number of H-bonds formed across dimer interface; (Salt) the number of salt bridges formed across dimer interface.

Table 3
DALI search results of structurally related proteins.

Protein	*Z*-score[a]	RMSD[a]	%ID[a]
2F2E	12.7	3.8	38
2YR2	11.5	3.3	15
3BPV	11.2	3.6	16
2HZT	11.1	2.5	29
4A5M	11.0	2.7	27

[a] Column headings refer to the following: (*Z*-score) similarity score from DALI; (RMSD) root mean square deviations; (%ID) % sequence identity with PA1374.

noteworthy that only PA1374 and 2F2E contained β-sheet in the dimer interface, whereas other proteins were mostly α-helical and contained β-sheet only in the wHTH region.

3.3. Hydrophobic pocket near the conserved Cys

A pocket with a size of 209 Å^3 calculated by the pocket-finder program [22] was observed in each monomer (Fig. 2). The pocket was formed mainly by hydrophobic residues, including Ile13, Leu17, Trp23, Ile26, Leu27, Arg30, Leu33, Gln34, Arg90, Leu93, Met94, Val 97, and Val111, from one subunit and Thr141, Val142, Met152, and Leu156 from the other subunit (Fig. 1C, purple arrows). Among these residues, Leu17, Trp23, Leu27, and Arg30 were completely conserved, whereas eight others were replaced by similar hydrophobic residues. Residues such as Leu33, Gln34, and Arg90 formed the opening of the pocket (indicated with an arrow in Fig. 2A and B). Interestingly, highly conserved Cys11 was located at one end of the pocket. In other MarR family transcription factors, a conserved cysteine residue close to the N-terminus is shown to undergo oxidation that leads to large conformational changes and plays an important role in the oxidative-stress sensing mechanism [6]. Hydrophobic pocket close to the oxidation-sensitive cysteine was observed in other OhrR family proteins and implicated in OHP binding [2,6]. Comparison of these hydrophobic pockets showed that the shape and size are quite variable and PA1374 contained the largest pocket with a length of approximately 14 Å and diameters of 9 Å and 4 Å in the wide and narrow part, respectively (Supplementary Fig. 2). This dumbbell-shaped pocket of PA1374 is large enough to encompass most part of linoleic acid (cis, cis-9, 12-octadecadienoic acid) when modeled in the pocket (Supplementary Fig. 2). Although PA1374 contains another cysteine residue (Cys140) in its C-terminal region, it is located on the other side with distances to Cys11 (same subunit) and Cys11′ (other subunit) of 32 Å and 23 Å, respectively, which makes the formation of intra- or inter-subunit disulfide bonds unlikely. Therefore, PA1374 could be a member of the 1-cysteine OhrR family.

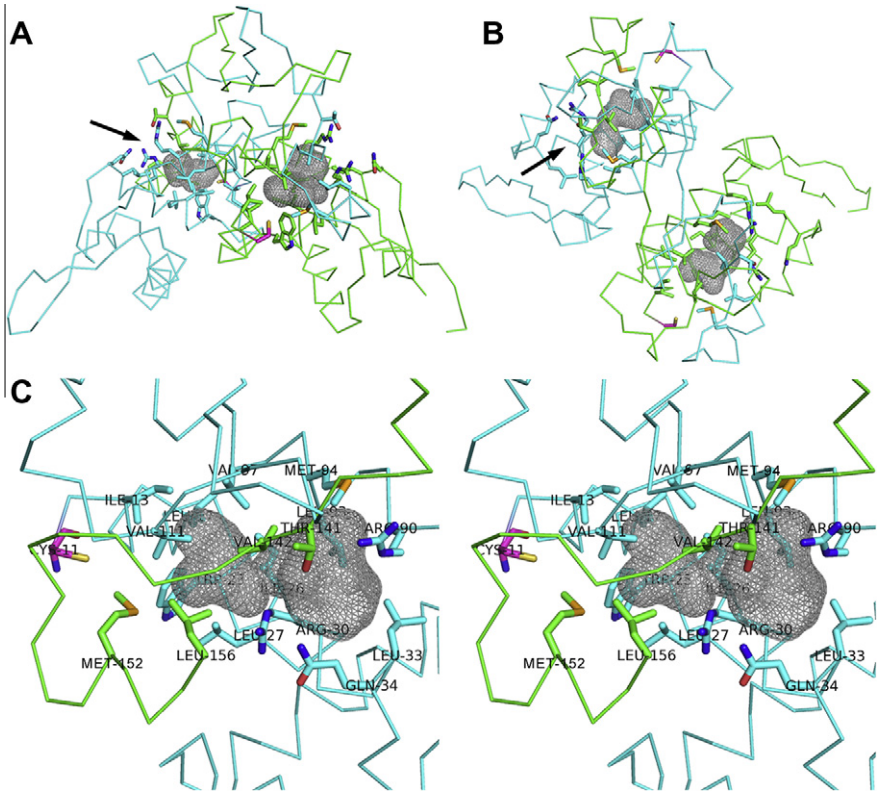

Fig. 2. The hydrophobic pockets near the conserved cysteine 11. (A) The ribbon representation of PA1374 dimer with the pockets in each subunit shown in mesh. Residues forming the pocket are shown as ball-and-stick and the opening of the pocket is indicated with an arrow. (B) 90° rotated (top view) of (A). (C) Stereoview of the pocket. Pocket is shown in grey mesh and the highly conserved cysteine that can undergo oxidation is shown as pink ball-and-stick.

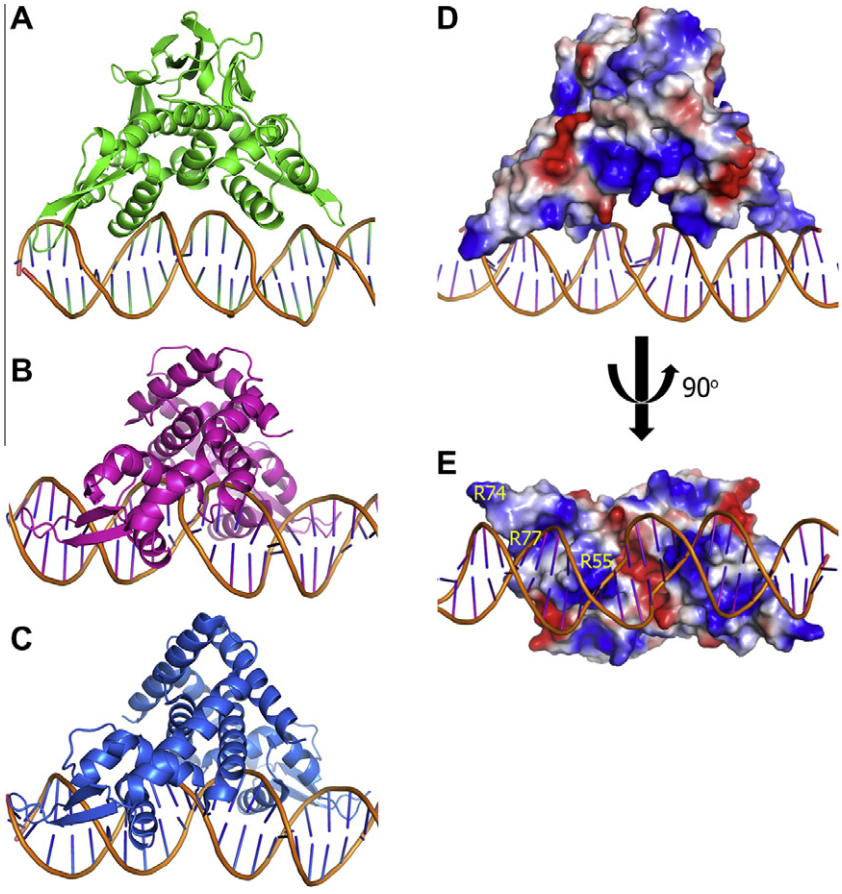

Fig. 3. Model of PA1374-DNA complex. (A) Model of PA1374 dimer binding to double stranded DNA (B) crystal structure of OhrR-ohrA operator complex (PDB ID: 1Z9C) (C) structure of SlyA-DNA complex (3Q5F) (D). PA1374 is shown as an electrostatic potential of the molecular surface. The basic regions are shown in blue, and the acidic regions in red. (E) 90° rotated (bottom view) of (D). The positions of conserved arginines (Arg55, Arg74 and Arg77) are indicated.

3.4. PA1374 and DNA binding

The structures of MarR family proteins with operator DNA have demonstrated that dimers bind to DNA [15,23]. To determine whether or not PA1374 has the appropriate size and properties to bind to DNA, we modeled PA1374 in complex with B-form DNA using energy minimization method [24] (Fig. 3A). One of the common interactions observed in the previous structures is the insertion of the recognition helix (α4) of the HTH motif into the major groove of DNA, and another interaction is between the tip of the wing and the minor groove of DNA (Fig. 3B and C). In these complex structures, conserved arginine residues were shown to play major role in the interaction with DNA [15,23]. The model of PA1374-DNA complex showed that the α4 recognition helix and wing of the PA1374 dimer had the right dimensions to interact with the major and minor grooves of DNA, respectively (Fig. 3A). These DNA-binding elements (the recognition helix and wing region of wHTH motif) also contained very well conserved Arg residues such as Arg55 in helix α4 and Arg74 and Arg77 in the wing (Fig. 1C, blue arrows), which can interact with a negatively charged DNA (Fig. 3D and E). Although the exact orientations of DNA-binding elements of PA1374 in this model are different from other structures shown in Fig. 3, PA1374 might undergo conformational changes for binding to DNA as often shown in other MarR family proteins [15,16,23].

In summary, PA1374 is a homodimer with a winged helix–turn–helix motif adopted by other transcriptional repressors such as MarR family proteins. The DNA-binding elements of the wHTH motif, including the α4 recognition helix and the wing, contain conserved Arg residues that can potentially interact with DNA. The presence of a hydrophobic pocket near the highly conserved Cys11 suggests that PA1374 might respond to oxidative stress induced by OHPs through oxidation of Cys11. However, further biochemical experiments are required to elucidate the exact role and regulation mechanisms.

Acknowledgments

We thank the staff members of Photon Factory beamline BL-5A for assistance in data collection. This research was supported by Basic Science Research Program through the National Research Foundation of Korea (NRF) funded by the Ministry of Education, Science and Technology (Grant number: MEST, R01-2010-0011364).

Appendix A. Supplementary data

Supplementary data associated with this article can be found, in the online version, at http://dx.doi.org/10.1016/j.bbrc.2013.01.044.

References

[1] H. Antelmann, J.D. Helmann, Thiol-based redox switches and gene regulation, Antioxid. Redox Signal. 14 (2011) 1049–1063.
[2] G.J. Palm, B. Khanh Chi, P. Waack, K. Gronau, D. Becher, D. Albrecht, W. Hinrichs, R.J. Read, H. Antelmann, Structural insights into the redox-switch mechanism of the MarR/DUF24-type regulator HypR, Nucleic Acids Res. 40 (2012) 4178–4192.
[3] P.R. Chen, P. Brugarolas, C. He, Redox signaling in human pathogens, Antioxid. Redox Signal. 14 (2011) 1107–1118.

[4] M. Fuangthong, J.D. Helmann, The OhrR repressor senses organic hydroperoxides by reversible formation of a cysteine–sulfenic acid derivative, Proc. Natl. Acad. Sci. USA 99 (2002) 6690–6695.

[5] M. Fuangthong, S. Atichartpongkul, S. Mongkolsuk, J.D. Helmann, OhrR is a repressor of ohrA, a key organic hydroperoxide resistance determinant in *Bacillus subtilis*, J. Bacteriol. 183 (2001) 4134–4141.

[6] K.J. Newberry, M. Fuangthong, W. Panmanee, S. Mongkolsuk, R.G. Brennan, Structural mechanism of organic hydroperoxide induction of the transcription regulator OhrR, Mol. Cell 28 (2007) 652–664.

[7] J.R. Cussiol, S.V. Alves, M.A. de Oliveira, L.E. Netto, Organic hydroperoxide resistance gene encodes a thiol-dependent peroxidase, J. Biol. Chem. 278 (2003) 11570–11578.

[8] J. Lesniak, W.A. Barton, D.B. Nikolov, Structural and functional characterization of the Pseudomonas hydroperoxide resistance protein Ohr, EMBO J. 21 (2002) 6649–6659.

[9] J.W. Lee, S. Soonsanga, J.D. Helmann, A complex thiolate switch regulates the *Bacillus subtilis* organic peroxide sensor OhrR, Proc. Natl. Acad. Sci. USA 104 (2007) 8743–8748.

[10] Z. Otwinowski, W. Minor, Processing of X-ray Diffraction Data Collected in Oscillation Mode, Methods Enzymol. 276 (1997) 307–326.

[11] P.D. Adams, P.V. Afonine, G. Bunkoczi, V.B. Chen, I.W. Davis, N. Echols, J.J. Headd, L.W. Hung, G.J. Kapral, R.W. Grosse-Kunstleve, A.J. McCoy, N.W. Moriarty, R. Oeffner, R.J. Read, D.C. Richardson, J.S. Richardson, T.C. Terwilliger, P.H. Zwart, PHENIX: a comprehensive Python-based system for macromolecular structure solution, Acta Crystallogr. D Biol. Crystallogr. 66 (2010) 213–221.

[12] G.N. Murshudov, A.A. Vagin, E.J. Dodson, Refinement of macromolecular structures by the maximum-likelihood method, Acta Crystallogr. D Biol. Crystallogr. 53 (1997) 240–255.

[13] P. Emsley, B. Lohkamp, W.G. Scott, K. Cowtan, Features and development of Coot, Acta Crystallogr. D Biol. Crystallogr. 66 (2010) 486–501.

[14] R.A. Laskowski, M.W. Macarthur, D.S. Moss, J.M. Thornton, Procheck – a program to check the stereochemical quality of protein structures, J. Appl. Crystallogr. 26 (1993) 283–291.

[15] M. Hong, M. Fuangthong, J.D. Helmann, R.G. Brennan, Structure of an OhrR-ohrA operator complex reveals the DNA binding mechanism of the MarR family, Mol. Cell 20 (2005) 131–141.

[16] T. Kumarevel, T. Tanaka, T. Umehara, S. Yokoyama, ST1710-DNA complex crystal structure reveals the DNA binding mechanism of the MarR family of regulators, Nucleic Acids Res. 37 (2009) 4723–4735.

[17] W. Kabsch, C. Sander, Dictionary of protein secondary structure: pattern recognition of hydrogen-bonded and geometrical features, Biopolymers 22 (1983) 2577–2637.

[18] E. Krissinel, K. Henrick, Inference of macromolecular assemblies from crystalline state, J. Mol. Biol. 372 (2007) 774–797.

[19] L. Holm, P. Rosenstrom, Dali server: conservation mapping in 3D, Nucleic Acids Res. 38 (2010) W545–549.

[20] E.A. Sieminska, X. Xu, A. Savchenko, D.A. Sanders, The X-ray crystal structure of PA1607 from *Pseudomonas aureginosa* at 1.9 Å resolution–a putative transcription factor, Protein Sci. 16 (2007) 543–549.

[21] V. Saridakis, D. Shahinas, X. Xu, D. Christendat, Structural insight on the mechanism of regulation of the MarR family of proteins: high-resolution crystal structure of a transcriptional repressor from Methanobacterium thermoautotrophicum, J. Mol. Biol. 377 (2008) 655–667.

[22] M. Hendlich, F. Rippmann, G. Barnickel, LIGSITE automatic and efficient detection of potential small molecule-binding sites in proteins, J. Mol. Graph. Model. 15 (1997) 359–363. 389.

[23] K.T. Dolan, E.M. Duguid, C. He, Crystal structures of SlyA protein, a master virulence regulator of *Salmonella*, in free and DNA-bound states, J. Biol. Chem. 286 (2011) 22178–22185.

[24] E. Krieger, K. Joo, J. Lee, S. Raman, J. Thompson, M. Tyka, D. Baker, K. Karplus, Improving physical realism, stereochemistry, and side-chain accuracy in homology modeling: four approaches that performed well in CASP8, Proteins 77 (Suppl. 9) (2009) 114–122.